# Spectroscopic Studies on the Interaction of the Antibiotic Lasalocid A (X537A) with Lanthanide(III) Ions in Methanol

**Frederick S. Richardson* and Anupam Das Gupta**

*Contribution from the Department of Chemistry, University of Virginia, Charlottesville, Virginia 22901.* *Received August 25, 1980*

**Abstract:** Interactions between trivalent lanthanide ions ($Ln^{3+}$) and the anionic form of the ionophore lasalocid A ($X537A^-$) in methanol and methanol–water solutions are investigated by using a variety of electronic absorption and emission spectroscopic techniques. The quenching of intrinsic lasalocid fluorescence by $Ln^{3+}$ ions is studied as a function of $[Ln^{3+}]/[X^-]$ (where $X^-$ denotes the lasalocid anion) for $Ln^{3+} = Pr^{3+}$, $Nd^{3+}$, $Eu^{3+}$, $Gd^{3+}$, and $Tb^{3+}$. The enhancement of terbium luminescence under near-ultraviolet excitation via lasalocid-to-$Tb^{3+}$ nonradiative energy-transfer processes is studied as a function of $[X^-]/[Tb^{3+}]$. Circular polarization of luminescence (CPL) measurements are reported for terbium–lasalocid systems of variable $[X^-]/[Tb^{3+}]$ to probe the interactions between bound $Tb^{3+}$ and the chiral centers of the lasalocid ligand. The absorption intensities of the hypersensitive $^4I_{9/2} \rightarrow {}^4G_{5/2}$ and $^4G_{7/2}$ $Nd^{3+}$ transitions are measured as a function of $[X^-]/[Nd^{3+}]$ to probe $Nd^{3+}$–lasalocid complex formation. The combined absorption, fluorescence quenching, CPL, and terbium luminescence intensity results conclusively demonstrate lanthanide–lasalocid complexation and provide clues and qualitative information regarding the structures and stoichiometries of the complexes formed in methanol solution. Results obtained on $X^-/Ln^{3+}/Ca^{2+}$ systems show that the $Ln^{3+}$ ions bind much more strongly than do $Ca^{2+}$ ions and apparently prevent (or interfere with) $Ca^{2+}$ binding to lasalocid. Studies on $X^-$/EDTA/$Ln^{3+}$ systems show that $Ln^{3+}$–$X^-$ binding persists in the presence of EDTA, although the structural features of the complexes are different from those formed in the absence of EDTA. The influence of water and the relative effects of $Cl^-$ vs. $NO_3^-$ anions in the $X^-/Ln^{3+}$ methanol solutions are investigated and analyzed with respect to both structural and spectroscopic considerations. Spectroscopic results are also reported for $Tb^{3+}$–salicylic acid systems in methanol.

The antibiotic lasalocid A (X537A) is a known ionophore for both monovalent and divalent cations. Its metal complexes are highly soluble in nonpolar solvents and are permeable through biological membranes. Numerous studies have been carried out on this ionophore and have emphasized various aspects of its biochemistry, chemical characterization, the equilibria and kinetics of its binding to metal ions, and the structural properties of the free ionophore and its metal complexes. The structural aspects of X537A and its metal complexes have been studied in the solid state by X-ray crystallography[1-7] and Raman spectroscopy,[8] and in solution by a variety of spectroscopic techniques including fluorescence,[9-13] circular dichroism,[10-13] Raman scattering,[8] and $^1H$ and $^{13}C$ NMR.[2,3,13-18] These latter studies have shown X537A to have extraordinary conformational flexibility, with conformational preference and stability being very sensitive to metal ion binding, the nature of the coordinated metal ions, solvent polarity and basicity, and the extent of deprotonation at the carboxyl group of the salicylic acid moiety.

The primary structure of lasalocid A (X537A) is shown below.

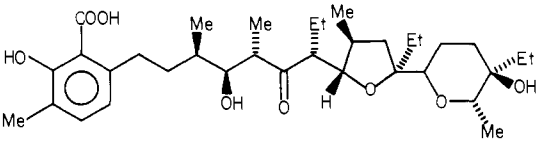


lasalocid A (X537A)

An examination of this structure immediately suggests that the metal binding propensity of X537A can be attributed to the presence of eight oxygen atoms, at least six of which can serve simultaneously as metal ligators. It is generally believed that in nonpolar solvents the ionophore encircles the cation to which it is coordinated and presents a hydrophobic external surface to the solvent medium. Steric considerations allow such a structure to be formed via six cation–oxygen linkages. In this structure, only two of the eight oxygen atoms in the X537A molecule are excluded from the inner coordination sphere of the cation. These nonligating oxygens are the carbonyl oxygen of the salicylic acid group and the phenolic oxygen of the same moiety. In highly polar solvents where the solvent molecules can strongly solvate the cation, it is unlikely that such a "tight", six-coordinate complex will be stable. However, under conditions in which the salicylic acid carboxyl and/or phenolic groups are deprotonated, it is likely that at least unidentate or bidentate cation-X537A coordination will occur.

In all of the spectroscopic studies reported to date on X537A and its metal complexes, the spectroscopic observables have been associated with atoms or groups within the ionophore itself. In the NMR experiments, the $^1H$ and $^{13}C$ nuclei served as intrinsic magnetic probes; in the absorption/CD experiments, the carbonyl and salicylic acid moieties served as near-ultraviolet absorptive chromophores; and in the fluorescence experiments, the salicylic acid moiety served as an intrinsic fluorophore. In all of the reported studies on metal ion complexes of X537A, the metal ions were treated as spectroscopically passive except insofar as they perturbed the spectroscopic properties of the intrinsic probes via metal ion induced conformational changes or metal ion–$^1H$ and metal ion–$^{13}C$ magnetic interactions.

In the present study, we examine the interactions of trivalent lanthanide ions ($Ln^{3+}$) with the basic form of X537A in pure methanol (MeOH) solvent and methanol–water (MeOH–$H_2O$)

(1) Westley, J. W.; Blount, J. F.; Evans, R. H.; Stempel, A.; Berger, J. *J. Antibiot.* **1974**, *27*, 597.
(2) Chiang, C. C.; Paul, I. C. *Science (Washington, DC)* **1977**, *196*, 1441.
(3) Schmidt, P. G.; Wang, A.; Paul, I. C. *J. Am. Chem. Soc.* **1974**, *96*, 6189.
(4) Bissell, E. C.; Paul, I. C. *J. Chem. Soc., Chem. Commun.* **1972**, 967.
(5) Maier, C. A.; Paul, I. C. *J. Chem. Soc., Chem. Commun.* **1971**, 181.
(6) Johnson, S. M.; Herrin, J.; Liu, S. J.; Paul, I. C. *J. Am. Chem. Soc.* **1970**, *92*, 4428.
(7) Johnson, S. M.; Herrin, J.; Liu, S. J.; Paul, I. C. *J. Chem. Soc., Chem. Commun.* **1970**, 72.
(8) Phillies, G. D. J.; Stanley, H. E. *J. Am. Chem. Soc.* **1976**, *98*, 3892.
(9) Haynes, D. H.; Pressman, B. C. *J. Membr. Biol.* **1974**, *16*, 195.
(10) Degani, H.; Friedman, H. L. *Biochemistry* **1974**, *13*, 5022.
(11) Cornelius, G.; Gartner, W.; Haynes, D. H. *Biochemistry* **1974**, *13*, 3052.
(12) Alpha, S. R.; Brady, A. H. *J. Am. Chem. Soc.* **1973**, *95*, 7043.
(13) Chen, S.-T.; Springer, C. S. *Bioinorg. Chem.* **1978**, *9*, 101.
(14) Westley, J. W.; Pruess, D. L.; Pitcher, R. G. *J. Chem. Soc., Chem. Commun.* **1972**, 161.
(15) Shen, C.; Patel, D. J. *Proc. Natl. Acad. Sci. U.S.A.* **1976**, *73*, 4277.
(16) Patel, D. J.; Shen, C. *Proc. Natl. Acad. Sci. U.S.A.* **1976**, *73*, 1786.
(17) Anteunis, M. J. O. *Bioorg. Chem.* **1976**, *5*, 327.
(18) Westley, J. W.; Evans, R. H.; Williams, T.; Stempel, A. *J. Chem. Soc., Chem. Commun.* **1970**, 71.

0002-7863/81/1503-5716$01.25/0 

mixtures. Although the $Ln^{3+}$ ions are of no *direct* physiological interest, it has been shown that they can be used to great advantage as spectroscopically active substitutional probes for physiological $Ca^{2+}$ and $Mg^{2+}$ in biomolecular systems.[19-21] Except for the generally stronger binding constants exhibited by $Ln^{3+}$ ions vs. $Ca^{2+}$ and $Mg^{2+}$, the coordination chemistries of $Ln^{3+}$, $Ca^{2+}$, and $Mg^{2+}$ ions are quite similar. The advantages offered by $Ln^{3+}$-for-$Ca^{2+}$ (or $Mg^{2+}$) replacement are the paramagnetic properties of the $Ln^{3+}$ ions and the optical spectroscopic properties of many of the $Ln^{3+}$ ions. It is already known that the X537A ionophore is able to transport $Pr^{3+}$ across phospholipid bilayer membranes[22,23] and between the aqueous cores of phospholipid inverse micelles.[13] Furthermore, Chen and Springer[13] have recently reported a detailed study of $Pr^{3+}$–X537A binding in MeOH using X537A fluorescence, circular dichroism, and $^1H$ and $^{13}C$ NMR spectroscopy and have related their results to the probable structural characteristics of the physiological $Ca^{2+}$–ionophore X537A complexes.

In the experiments reported here, optical absorption and emission spectroscopic measurements were used to probe the $Ln^{3+}$–X537A interactions in MeOH and MeOH–$H_2O$ solutions. $Tb^{3+}$ and $Eu^{3+}$ were employed as "active" spectroscopic probes by monitoring their total luminescence (TL) and circularly polarized luminescence (CPL) spectra and as "passive" spectroscopic probes by monitoring their quenching effects on the intrinsic X537A fluorescence. Other, nonluminescent, $Ln^{3+}$ ions were employed as quenchers of intrinsic X537A fluorescence. Near-ultraviolet excitation spectra of both X537A fluorescence and (bound) $Tb^{3+}$ luminescence were used to study the nonradiative transfer of excitation from the salicylate moiety of the ionophore to the bound $Tb^{3+}$ ions. The "hypersensitive" $^4I_{9/2} \rightarrow {}^4G_{5/2}$ absorptive transition of $Nd^{3+}$ was used to probe $Nd^{3+}$–X537A complex formation. Furthermore, parallel studies were carried out by using $LnCl_3$ and $Ln(NO_3)_3$ salts to check for the possible influence of anion effects.

Among the spectroscopic techniques employed in this study, the two most sensitive to the subtleties of $Ln^{3+}$–X537A binding and structure are $Tb^{3+}$ CPL and sensitization of $Tb^{3+}$ luminescence via energy transfer from the salicylate chromophore of X537A to bound $Tb^{3+}$. Both of these techniques have been used to great advantage in previous studies on the binding of $Tb^{3+}$ to chiral ligands which possess a near-ultraviolet chromophoric group (for example, protein molecules with aromatic side chain chromophores).[21,24-27] CPL is the emission analogue of circular dichroism and exhibits sensitivity to the same aspects of molecular structure as does CD.[26,27] In general, the major prerequisites for strong CPL from optically active $Tb^{3+}$ complexes are (1) strong $Tb^{3+}$–ligand binding involving multidentate chelation and (2) close proximity of the $Tb^{3+}$ ion to chiral features of the ligand environment. Previous studies on sensitization of $Tb^{3+}$ luminescence via intramolecular ("intracomplex") energy-transfer processes have revealed that this mechanism of $Tb^{3+}$ excitation is efficient only when the donor moiety is coordinated to, or lies very close to, the $Tb^{3+}$ acceptor ion.[24,28]

The most intense $Tb^{3+}$ luminescence is from the $^5D_4 \rightarrow {}^7F_5$ transition centered around 545 nm in MeOH solution. This transition was used as the principal probe transition in our CPL/luminescence studies involving $Tb^{3+}$.

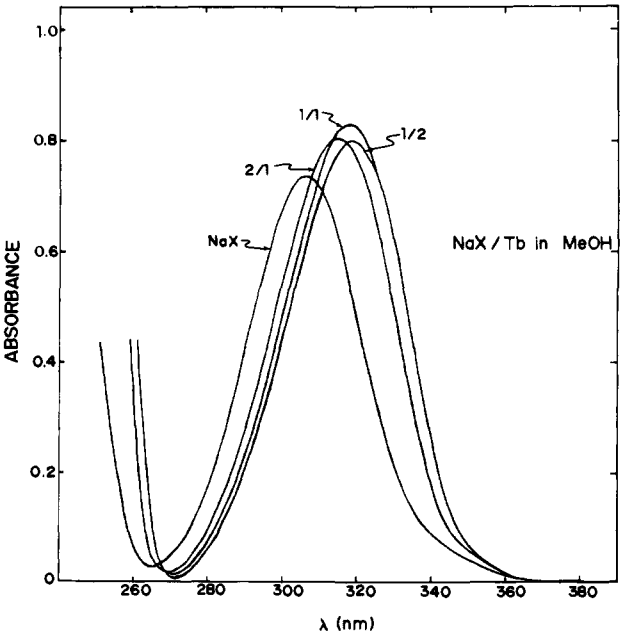


**Figure 1.** Near-ultraviolet absorption spectra for NaX, 2:1 NaX/Tb, 1:1 NaX/Tb, and 1:2 NaX/Tb in pure methanol using a fixed [NaX] = 0.125 mM and an optical path length of 1 cm.

## Experimental Section

The sodium salt of lasalocid A (X537A) was purchased from Aldrich Chemical Co. and was used without further purification. Spectral grade methanol, purchased from Mallinckrodt, was used in all of our experiments. The $LnCl_3$ and $Ln(NO_3)_3$ salts (99.999% purity) were either purchased directly from Alfa Inorganics or prepared from the oxides using standard procedures. Stock solutions of the sodium salt of X537A in pure, anhydrous MeOH were found to be stable over long periods of time (weeks) at room temperature. The anionic X537A in MeOH–$H_2O$ mixtures, however, was found to be relatively unstable, and fresh solutions had to be prepared on a daily or hourly basis for use in the spectroscopic experiments. The concentrations and compositions of all X537A/solvent solutions were checked by near-ultraviolet absorption measurements.

All absorption measurements were carried out at room temperature by using Cary 11 and Cary 17 spectrophotometers. Corrected excitation and emission spectra were obtained on a SLM Model 8000 emission spectrophotometer interfaced with a Hewlett–Packard Model 9815A calculator and a Hewlett–Packard Model 7225A plotter. A triangular quartz emission cuvette was used in these experiments, with emission viewed at right angles to excitation. Quantum yields of X537A fluorescence were determined according to the methods described by Demas and Crosby,[29] using $4 \times 10^{-2}$ mM quinine sulfate solution as a standard.

All CPL measurements were carried out by using an emission spectrophotometer constructed in this laboratory.[26,27] A 1000-W Xe–Hg arc lamp was used as a light source, and emission was detected at 180° to excitation. CPL and total luminescence intensity spectra were recorded simultaneously. The recorded CPL intensities are proportional to $\Delta I = I_L - I_R$, where $I_{L(R)}$ is the intensity of the left (right) circularly polarized component of the luminescence. The total luminescence intensity is proportional to $I = (I_L + I_R)/2$. Both $\Delta I$ and $I$ are given in relative (and arbitrary) intensity units, but the ratio $\Delta I/I$ is given in absolute units. We shall refer to $\Delta I/I$ as the luminescence dissymmetry factor, denoted by $g_{lum}$. The luminescence dissymmetry factor has the same significance in CPL/luminescence spectroscopy as the ratio $\Delta\epsilon/\epsilon$ has in CD/absorption spectroscopy.[27]

## Results

All of our experiments were carried out on the sodium salt of X537A dissolved in pure MeOH or MeOH–$H_2O$ mixtures. Throughout the remainder of this paper we shall denote the Na (X537A) solute as NaX. When a trivalent $Ln^{3+}$ ion is also present in solution, we shall denote the *collection* of solute species present by NaX/Ln. This notation is *not* meant to connote anything regarding the existence or nonexistence of stable complexes nor

(19) Nieboer, E. *Struct. Bonding (Berlin)* **1975**, *22*, 1.
(20) Reuben, J. In "Handbook on the Physics and Chemistry of Rare Earths"; Gschneidner, K. A., Jr., Eyring, L., Eds.; North-Holland Publishing Co.: Amsterdam, 1979; Chapter 39.
(21) Martin, R. B.; Richardson, F. S. *Q. Rev. Biophys.* **1979**, *12*, 181.
(22) Fernandez, M. S.; Celis, H.; Montal, M. *Biochem. Biophys. Acta* **1973**, *323*, 600.
(23) Hunt, G. R. A. *FEBS Lett.* **1975**, *58*, 194.
(24) Brittain, H. G.; Richardson, F. S.; Martin, R. B. *J. Am. Chem. Soc.* **1976**, *98*, 8255.
(25) Steinberg, I. Z. *Annu. Rev. Biophys. Bioeng.* **1978**, *7*, 113.
(26) Richardson, F. S.; Riehl, J. P. *Chem. Rev.* **1977**, *77*, 773.
(27) Richardson, F. S. In "Optical Activity and Chiral Discrimination"; Mason, S. F., Ed.; D. Reidel Publishing Co.: Boston, 1979; Chapter 8, pp 189–219.
(28) Salama, S.; Richardson, F. S. *Inorg. Chem.* **1980**, *19*, 635.
(29) Demas, J. N.; Crosby, G. A. *J. Phys. Chem.* **1971**, *75*, 991.

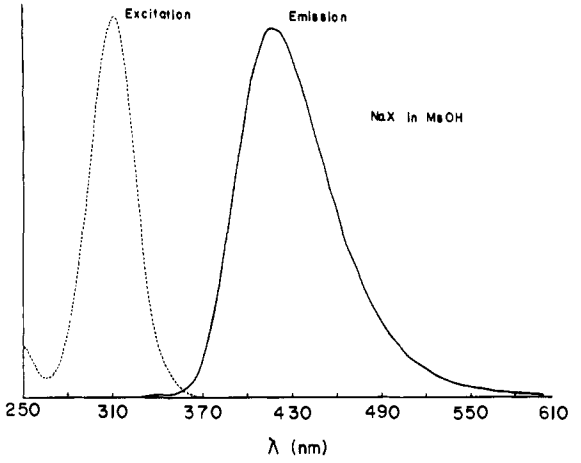


**Figure 2.** Corrected excitation and emission spectra for NaX in methanol. For the excitation measurements emission was monitored at 420 nm, and in the emission measurements excitation was at 310 nm ($\Delta\lambda_{ex} \simeq 20$ nm). In both sets of measurements sample absorbance was 0.16 at 310 nm, and a triangular fluorescence cuvette was used with a 90° (right-angle) excitation–emission detection geometry.

does it reflect possible stoichiometries for existing complexes. Molar concentration ratios of NaX to $Ln^{3+}$ are denoted by [NaX]/[Ln]. Free salicylic acid in solution is denoted by Sal, and salicylic acid in solution with trivalent lanthanide ions is denoted by Sal/Ln.

**Near-Ultraviolet Absorption Spectra.** The near-ultraviolet absorption spectra of NaX, 2:1 NaX/Tb, 1:1 NaX/Tb, and 1:2 NaX/Tb in methanol are shown in Figure 1. The NaX/Tb solutions were prepared by using $TbCl_3$. The near-ultraviolet spectra obtained on NaX/Tb solutions prepared from $Tb(NO_3)_3$ were found to be identical with the spectra shown in Figure 1. Although red shifted upon addition of $Tb^{3+}$, the integrated band intensity of the NaX near-ultraviolet absorption remains relatively unaffected by the presence of $Tb^{3+}$. Since $Tb^{3+}$ exhibits only very weak absorption ($\epsilon < 10$) in the 280–360-nm region, the observed changes in the NaX spectrum upon addition of $Tb^{3+}$ may be attributed to $Tb^{3+}$-induced perturbations on the salicylic acid chromophore of the lasalocid molecule.

**NaX Excitation and Emission Spectra.** Corrected excitation and emission spectra for NaX in methanol are shown in Figure 2. The quantum yield of the lasalocid fluorescence was determined to be 0.15.

**NaX/Ln Excitation and Emission Spectra.** A variety of excitation and emission measurements were carried out on NaX/Ln systems in methanol solution. The principal objectives of these measurements were to (a) investigate the influence of various lanthanide ions as quenchers of lasalocid fluorescence and (b) investigate the sensitization of lanthanide luminescence via energy transfer from lasalocid (as donor) to a lanthanide ion (serving as the acceptor). The lanthanide ions included in these studies were $Pr^{3+}$, $Nd^{3+}$, $Gd^{3+}$, $Eu^{3+}$, and $Tb^{3+}$, and separate studies were conducted by using the $LnCl_3$ and $Ln(NO_3)_3$ salts to check for possible anion effects.

In the quenching experiments, broad-band excitation ($\Delta\lambda_{ex} \sim 20$ nm) centered around 310 nm was used on samples of constant absorbance (at the excitation maximum). The entire lasalocid emission spectrum was recorded in each experiment, and the integrated intensity of this spectrum was determined. The samples in these experiments were composed of NaX/Ln in methanol with variable [NaX]/[Ln] concentration ratios but with the NaX concentration held fixed at $4 \times 10^{-2}$ mM. The percent quenching of lasalocid fluorescence by added lanthanides was calculated according to

$$\% Q = 100(F_0 - F)/F_0, \quad (1)$$

where $F_0$ is the integrated fluorescence intensity of pure NaX in methanol and $F$ is the integrated fluorescence intensity of lasalocid in methanol solutions of NaX/Ln. Denoting [NaX]/[Ln] by $\chi$,

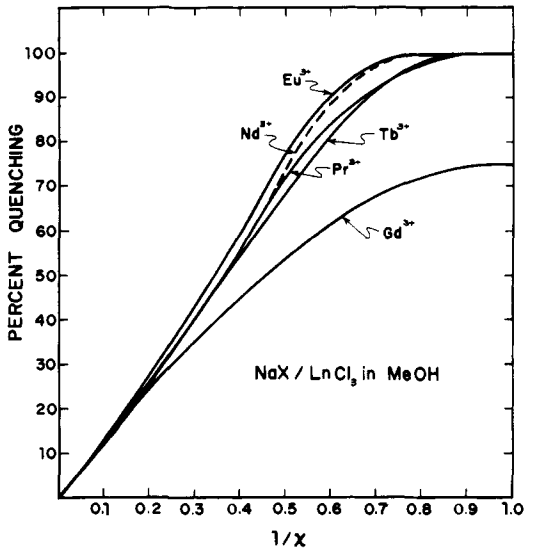


**Figure 3.** Percent quenching (% $Q$) of lasalocid fluorescence vs. $1/\chi$ = [Ln]/[NaX] for NaX/Ln in methanol. The [NaX] concentration was held fixed at $4 \times 10^{-2}$ mM and excitation was centered around 310 nm ($\Delta\lambda_{ex} \simeq 20$ nm) on samples of constant absorbance. The lanthanides were introduced into solution as trichloride salts.

Table I. Percent Quenching of Lasalocid Fluorescence (% $Q$) by Lanthanide Ions for $\chi = 1$ and $\chi = 2$

| | % $Q$ | |
|---|---|---|
| $Ln^{3+}$ | $\chi = 1$ | $\chi = 2$ |
| $Pr^{3+}$ (chloride) | 100 | 72 |
| $Eu^{3+}$ (chloride) | 100 | 75 |
| $Nd^{3+}$ (chloride) | 100 | 74 |
| $Gd^{3+}$ (chloride) | 75 | 54 |
| $Tb^{3+}$ (chloride) | 100 | 69 |
| $Tb^{3+}$ (nitrate) | 100 | 69 |

$F$ was measured for 10 different values of $\chi$ by varying [Ln] and holding [NaX] constant. The % $Q$ values were then calculated from eq 1, and plots of % $Q$ vs. $1/\chi$ are shown in Figure 3 for $Ln^{3+} = Pr^{3+}$, $Eu^{3+}$, $Nd^{3+}$, $Gd^{3+}$, and $Tb^{3+}$. The accuracy and validity of this procedure for determining percent quenching of lasalocid fluorescence depends critically on (a) there being negligible lanthanide contribution to the near-ultraviolet excitation of the NaX/Ln system and (b) the absence of lanthanide ion emission in the region of lasalocid fluorescence (~360–580 nm). Both of these criteria are satisfied for $Pr^{3+}$, $Eu^{3+}$, $Nd^{3+}$, and $Gd^{3+}$. However, for $Tb^{3+}$ the second criterion is not satisfied since it was found that $Tb^{3+}$ emission overlaps the lasalocid fluorescence spectrum between approximately 490 and 580 nm. This overlap region makes only a small contribution to the overall lasalocid fluorescence; so its effect on the % $Q$ data for NaX/Tb is easy to correct for. Our corrections for this effect are reflected in the NaX/Tb data shown in Figure 3. All of the data presented in Figure 3 were obtained on solutions in which the lanthanides were dissolved as their trichloride salts. In Table I we present the values of % $Q$ corresponding to $\chi = 1$ and $\chi = 2$ for the various lanthanide ions in NaX/Ln methanol solutions.

Among the lanthanides investigated in the present study, only $Tb^{3+}$ and $Eu^{3+}$ were found to luminesce in methanol solution with and without lasalocid present. The $^5D_0 \rightarrow {}^7F_J$ visible region luminescence for $Eu^{3+}$ was found to be very weak, and this luminescence exhibited an excitation spectrum (throughout the near-ultraviolet and visible exciting wavelength regions) which was independent of the presence or absence of lasalocid. On the other hand, the $^5D_4 \rightarrow {}^7F_J$ terbium luminescence was found to be very strong (especially in the $^5D_4 \rightarrow {}^7F_5$ transition region), and its intensity under near-ultraviolet excitation was found to be strongly dependent upon lasalocid concentration. In fact, the near-ultraviolet excitation spectrum for $^5D_4 \rightarrow {}^7F_5$ terbium luminescence in NaX/Tb solutions exactly matches that of lasalocid

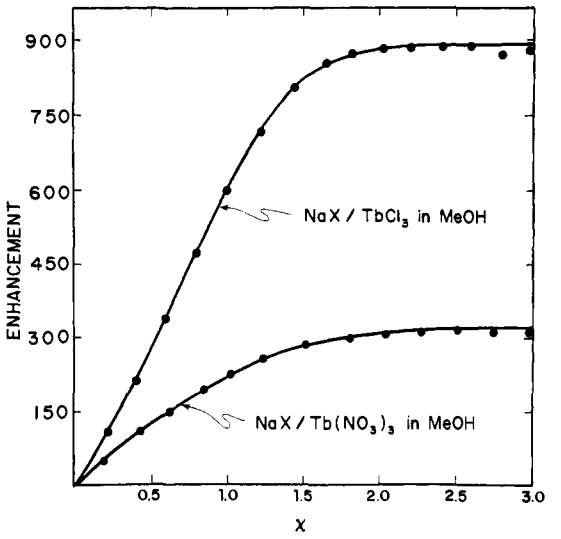


**Figure 4.** Terbium luminescence enhancement ($E$) vs. $\chi$ = [NaX]/Tb for $NaX/TbCl_3$ and $NaX/Tb(NO_3)_3$ in methanol solution. Excitation was into the near-ultraviolet lasalocid absorption band centered near 310 nm, and the terbium 535–555-nm luminescence intensity was measured. Enhancement ($E$) is defined by eq 2 in the text.

fluorescence (with respect to its band shape and $\lambda_{max}$). Furthermore, the terbium luminescence intensity from NaX/Tb vs. that from free $Tb^{3+}$ (in methanol) was found to be significantly stronger when excitation was into the 310-nm lasalocid absorption band. These results imply sensitization (and enhancement) of terbium luminescence from NaX/Tb solutions via a mechanism involving near-ultraviolet absorption by the salicylic acid moiety of the lasalocid molecule followed by nonradiative energy transfer from the salicylic acid chromophore to a $Tb^{3+}$ ion.

Our results on the sensitization of terbium luminescence by lasalocid-to-$Tb^{3+}$ energy transfer may be conveniently expressed in terms of terbium luminescence enhancement factors. Defining $I_0$ to be the integrated $^5D_4 \rightarrow {}^7F_5$ terbium luminescence intensity for "free" $Tb^{3+}$ in methanol solution under broad-band near-ultraviolet excitation centered around 310 nm, and defining $I$ to be the same quantity except that it is determined for NaX/Tb solutions of variable $\chi$, we may define an enhancement factor for terbium luminescence according to

$$E = (I - I_0)/I_0 \qquad (2)$$

Obviously, the $E$ defined by this equation may be either negative or positive, depending upon whether the lasalocid quenches or enhances the terbium luminescence intensity. The value of $E$ will be zero in certain limits where $\chi \rightarrow 0$ and/or $Tb^{3+}$–lasalocid interactions are negligible. Plots of $E$ vs. $\chi$ are shown in Figure 4 for the separate sets of experiments in which $TbCl_3$ and $Tb(NO_3)_3$ were used to prepare the NaX/Tb solutions. In determining the $I$ values in eq 2 for the $^5D_4 \rightarrow {}^7F_5$ terbium luminescence, it was necessary to subtract off the red tail of the residual lasalocid fluorescence (recalling that this red tail overlaps the 535–555-nm region where $^5D_4 \rightarrow {}^7F_5$ terbium emission occurs). This subtraction was made easy by the sharpness of the $^5D_4 \rightarrow {}^7F_5$ emission band. The dramatic differences in the $E$ vs. $\chi$ plots when $TbCl_3$ is used vs. when $Tb(NO_3)_3$ is used (Figure 4) strongly suggest that the nature of the anions in solution has an important influence on either the structures of the complexes formed or the details of the $Tb^{3+}$–lasalocid interactions (or on *both* of these factors).

**NaX/Tb CPL/Emission Spectra.** Circular polarization of luminescence (CPL) spectra were measured for 2:1, 1:1, and 1:2 methanol solutions of $NaX/TbCl_3$ and $NaX/Tb(NO_3)_3$. These spectra were recorded throughout the $^5D_4 \rightarrow {}^7F_6$, $^7F_5$, $^7F_4$, and $^7F_3$ emission regions of $Tb^{3+}$, with the $^5D_4 \rightarrow {}^7F_5$ emission (535–555 nm) exhibiting the largest CPL and total luminescence intensities. The CPL/emission spectra obtained by near-ultraviolet (~310 nm) vs. visible (488 nm) irradiation were qualitatively

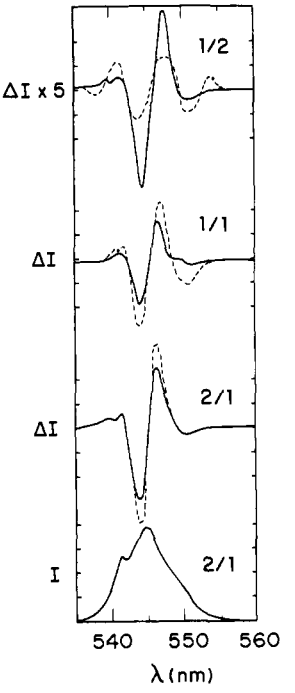


**Figure 5.** CPL/emission spectra in the $^5D_4 \rightarrow {}^7F_5$ terbium emission region for $NaX/Tb(NO_3)_3$ (solid line spectra) and $NaX/TbCl_3$ (dashed line spectra) in methanol with [NaX] = $4 \times 10^{-2}$ mM held constant. The spectra were obtained by using broad-band near-ultraviolet excitation centered at 310 nm. The ratios denote [NaX]/[Tb].

identical; but the CPL/emission intensities obtained by near-ultraviolet irradiation were observed to be at least an order-of-magnitude greater than those obtained with 488-nm excitation. This latter observation is a consequence of sensitization of terbium luminescence via lasalocid-to-$Tb^{3+}$ energy transfer when near-ultraviolet excitation is used. Excitation using the 488-nm line of an argon ion laser populates the $^5D_4$ emitting state of $Tb^{3+}$ directly by the $^5D_4 \leftarrow {}^7F_6$ absorptive transition. Even with ~1 W of laser power at 488 nm, this latter, *direct* excitation process is not as efficient as near-ultraviolet excitation owing to the very low absorptivity of the $^5D_4 \leftarrow {}^7F_6$ terbium transition. Near-ultraviolet excitation exploits the relatively strong lasalocid absorptivity in this region and the efficient lasalocid-to-$Tb^{3+}$ energy transfer.

CPL/emission spectra in the $^5D_4 \rightarrow {}^7F_5$ terbium emission region are shown in Figure 5. The CPL spectra are plotted as $\Delta I$ vs. $\lambda$, where $\Delta I = I_L - I_R$ and $I_L$ and $I_R$ denote, respectively, the intensities of the left and right circularly polarized components of the luminescence. The total luminescence intensity is plotted as $I$ vs. $\lambda$, where $I = (I_L + I_R)/2$. All of the spectra shown in Figure 5 were obtained by using broad-band near-ultraviolet excitation centered at 310 nm ($\Delta\lambda_{ex} \simeq 20$ nm) on samples with a fixed NaX concentration of $4 \times 10^{-2}$ mM. Common, but arbitrary, $\Delta I$ and $I$ intensity scales are used. Since these scales were not normalized to either a constant $Tb^{3+}$ ion concentration or a constant sample absorbance at the excitation wavelength, comparisons between the magnitudes of $\Delta I$ and $I$ for the various NaX/Tb systems must be confined to the *qualitative* features of the CPL/emission spectra. (Recall that the absorption $\lambda_{max}$ of the NaX/Tb systems is significantly red shifted from 310 nm as $\chi$ = [NaX]/[Tb] decreases—see Figure 1). A better quantitative basis for comparing the CPL/emission results on the various NaX/Tb systems is provided by the luminescence dissymmetry factors, $g_{lum} = \Delta I/I$, observed within the $^5D_4 \rightarrow {}^7F_5$ emission region. These factors are independent of sample absorbance and are independent of [Tb] for constant $\chi$. Values of $g_{lum}$ at 544 and 546 nm are listed in Table II for the $NaX/TbCl_3$ and $NaX/Tb(NO_3)_3$ systems.

Total luminescence spectra over the $^5D_4 \rightarrow {}^7F_6$ (485–500 nm), $^7F_5$ (535–555 nm), and $^7F_4$ (580–595 nm) terbium emission regions are presented in Figure 6 for the 2:1 $NaX/Tb(NO_3)_3$, 1:2

Table II. Luminescence Dissymmetry Factors Observed at 544 and 546 nm for NaX/Tb Systems in Methanol

| composition | $(\Delta I/I) \times 10^4$ λ = 546 nm | λ = 544 nm |
|---|---|---|
| | $NaX/TbCl_3$ | |
| 2:1 | 5.56 | −6.56 |
| 1:1 | 4.77 | −5.15 |
| 1:2 | 1.24 | −1.15 |
| | $NaX/Tb(NO_3)_3$ | |
| 2:1 | 4.11 | −4.93 |
| 1:1 | 3.01 | −3.55 |
| 1:2 | 2.47 | −2.89 |

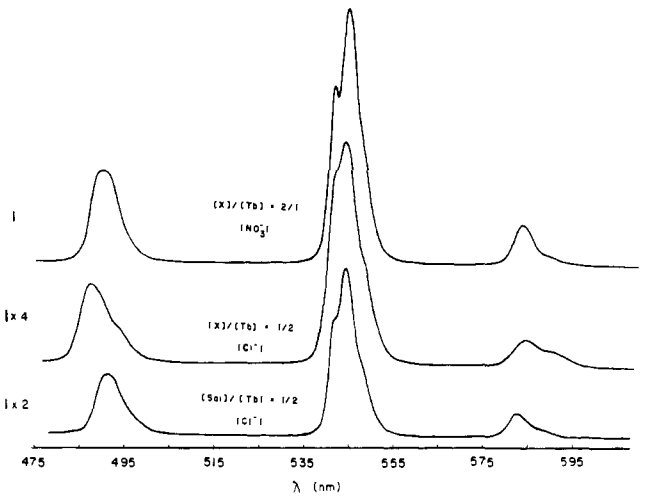


**Figure 6.** Total luminescence spectra in the $^5D_4 \rightarrow {}^7F_6$, $^7F_5$, and $^7F_4$ terbium emission regions for 2:1 $NaX/Tb(NO_3)_3$, 1:2 $NaX/TbCl_3$, and 1:2 $Sal/TbCl_3$ in methanol using broad-band near-ultraviolet excitation.

$NaX/TbCl_3$, and 1:2 $Sal/TbCl_3$ systems in methanol. These spectra were obtained with near-ultraviolet excitation of the ligands.

**NaX/Ca/Ln Emission Spectra.** Haynes and Pressman[9] have previously reported that complexation of $K^+$, $Ca^{2+}$, or $Ba^{2+}$ with anionic $X537A^-$ in solvents of high polarity tends to increase the intrinsic lasalocid fluorescence intensity, whereas such complexation in solvents of low polarity serves to decrease the lasalocid fluorescence. In the present study, we measured the integrated fluorescence intensity of NaX/Ca in methanol as a function of [Ca], holding [NaX] constant at $4 \times 10^{-2}$ mM, and found that the lasalocid fluorescence was enhanced in the presence of $Ca^{2+}$. This enhancement reached a maximum of about 5% at [NaX]/[Ca] = 1.

To check the competition of $Ln^{3+}$ ions for the $Ca^{2+}$ binding sites on the lasalocid ligands, we also measured the lasalocid fluorescence intensity as a function of [Ln] for 1:1:*n* NaX/Ca/Ln systems in methanol (where *n* denotes variable $Ln^{3+}$ concentrations). Plots of these data as % *Q* (defined by eq 1) vs. [Ln] revealed that for NaX/Ca/Ln = 1/1/*n*, with $n > 0.2$, the lasalocid fluorescence follows quenching curves which are nearly identical with those shown in Figure 3 for the NaX/Ln systems. These results suggest that the $Ln^{3+}$ and $Ca^{2+}$ ions are in competition for the same binding sites on the lasalocid ligands and that the $Ln^{3+}$ ions, with their greater positive charge, win the competition. Further evidence that $Ca^{2+}$ is probably not bound in the presence of significant $Ln^{3+}$ concentrations is the observation that 1:1:1 and 2:2:1 NaX/Ca/Tb systems exhibit near-ultraviolet excited CPL/emission spectra, in the $^5D_4 \rightarrow {}^7F_5$ terbium emission region, which are identical with those observed for the corresponding NaX/Tb systems.

**NaX/EDTA/Ln Emission Spectra.** It might be expected that the presence of another strong chelating ligand in solution would inhibit the $Ln^{3+}$–lasalocid interactions. To investigate this possibility, we examined the spectroscopic properties of a number of NaX/EDTA/Ln systems in methanol (EDTA = ethylenediaminetetraacetate anion). In aqueous solutions, EDTA is a strong chelating ligand for lanthanide ions and, when fully coordinated at neutral to basic pH values, it can occupy up to six coordination sites about the metal ion. The structures and coordination numbers of Ln(EDTA) complexes in methanol have not been characterized, but it seems likely that such complexes should be relatively stable and well formed. Introduced as an anion, EDTA presents four strongly coordinating carboxylate donor groups to a lanthanide ion, whereas anionic lasalocid presents only one carboxylate group plus a number of less strongly coordinating oxygen donor groups (ether oxygens, carbonyl oxygens, and hydroxyl groups).

Lasalocid fluorescence quenching experiments were carried out on a number of NaX/Ln(EDTA) systems in methanol in which [NaX] was held fixed at $4 \times 10^{-2}$ mM, [Ln]/[EDTA] was held fixed at 1, and [Ln(EDTA)] was varied from 0 to [NaX]. Over the range [Ln(EDTA)]/[NaX] = 0–1, the % *Q* vs. [Ln(EDTA)] plots for $Ln^{3+} = Pr^{3+}$, $Nd^{3+}$, $Eu^{3+}$, $Gd^{3+}$, and $Tb^{3+}$ were nearly identical with the equivalent % *Q* plots for the NaX/Ln systems. These results show that the 1:1 Ln(EDTA) complexes can quench lasalocid fluorescence with roughly the same efficiency as the free $Ln^{3+}$ ions.

CPL/emission spectra were also recorded for NaX/EDTA/Tb systems of variable concentration ratios. These spectra were obtained in the $^5D_4 \rightarrow {}^7F_5$ terbium emission region using near-ultraviolet excitation centered at 310 nm. For the 1:2:2 NaX/EDTA/Tb system, CPL was observed but was extremely weak. For the 1:1:1 system, the CPL intensity was somewhat stronger but was still weaker than that observed for the 1:1 NaX/Tb system. Only for the 1:1:2 system were CPL intensities and luminescence dissymmetry factors ($\Delta I/I$) observed to approach in magnitude the values measured for the corresponding NaX/Tb system. These CPL results on the NaX/EDTA/Tb systems suggest that EDTA binding to $Tb^{3+}$ does, in fact, interfere with or weaken $Tb^{3+}$–lasalocid coordination. Alternatively, it is possible that the reduced CPL intensities observed in the presence of EDTA can be attributed entirely to major changes in the cyrstal field wave functions of the $Tb^{3+}$ rather than to reduced $Tb^{3+}$–lasalocid binding.

All experiments on the NaX/EDTA/Ln systems were carried out by using lanthanide trichloride salts with methanol as the solvent.

**NaX/Nd Visible Absorption Spectra.** To further probe the interaction of lasalocid with lanthanide ions, we measured the integrated absorption intensity of the 555–590-nm absorption band of $Nd^{3+}$ as a function of [NaX] in methanol solutions of NaX/Nd. This absorption band in $Nd^{3+}$ complexes can be assigned to the $^4I_{9/2} \rightarrow {}^4G_{5/2}$ and $^4G_{7/2}$ 4f–4f transitions, both of which are members of the so-called "hypersensitive" class of lanthanide 4f–4f transitions. The lanthanide hypersensitive transitions are characterized by absorption intensities which are especially sensitive to the details of the ligand environment (e.g., the number and nature of donor atoms or groups, ligand geometry, and solvent medium). They are, therefore, useful probes of lanthanide–ligand complex formation and structure.

Our absorption measurements on the NaX/Nd methanol solutions were carried out on samples of fixed $[NdCl_3] = 10$ mM and variable [NaX]. Spectra for [NaX]/[Nd] = 0 and 1.5 are shown in Figure 7. Measurements were carried out on 16 different samples of varying [NaX], and the integrated band intensities were calculated for the 555–590-nm absorption. These integrated band intensities (expressed in arbitrary units) are plotted in Figure 8 vs. $\chi$ = [NaX]/[Nd]. These results clearly demonstrate rather strong $Nd^{3+}$–lasalocid interactions (binding) which are dependent upon the concentration ratio factor $\chi$.

**NaX/Tb Methanol–Water Solutions.** The structures of $Ln^{3+}$ (aquo) and $Ln^{3+}$ (methanolic) complexes are thought to be quite different,[30] and it is further believed that lasalocid conformation differs in aqueous vs. methanolic solutions. In the present study, a series of experiments were carried out on NaX/Tb systems in

(30) Yatsimirskii, K. B.; Davidenko, N. K. *Coord. Chem. Rev.* **1979**, *27*, 223.

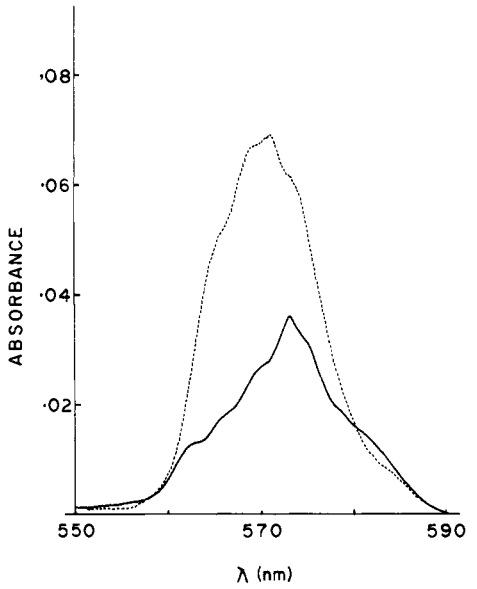


**Figure 7.** Absorption spectra for $NdCl_3$/methanol (solid curve) and 1.5:1 NaX/$NdCl_3$/methanol (broken curve) solutions. [$NdCl_3$] = 10 mM.

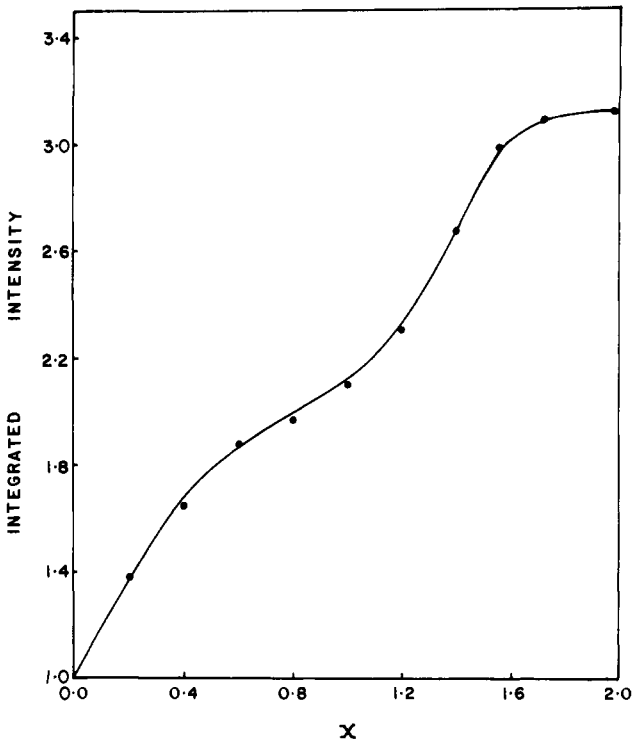


**Figure 8.** Integrated band intensity (expressed in arbitrary units) vs. $\chi$ = [NaX]/[Nd] for the 555–590-nm absorption of $Nd^{3+}$ in NaX/Nd methanol solution.

which lasalocid fluorescence quenching and terbium luminescence enhancement were determined in MeOH–$H_2O$ mixtures as a function of the MeOH–$H_2O$ concentration ratio. The $TbCl_3$ salt was used in these experiments, and fresh NaX/Tb MeOH–$H_2O$ solutions had to be prepared for each experiment since there appeared to be serious lasalocid decomposition in these samples under extended near-ultraviolet irradiation.

Plots of % $Q$ vs. $1/\chi$ = [Tb]/[NaX] and $E$ (terbium luminescence enhancement) vs. $\chi$ for NaX/Tb in MeOH–$H_2O$ mixtures were found to be qualitatively identical with the analogous plots for NaX/Tb in pure MeOH. Furthermore, the relationship between % $Q$ and $E$ as a function of $\chi$ was found to be closely similar for NaX/Tb in MeOH–$H_2O$ and pure MeOH. This latter observation suggests that the presence of water does not significantly influence the lasalocid-to-$Tb^{3+}$ energy-transfer

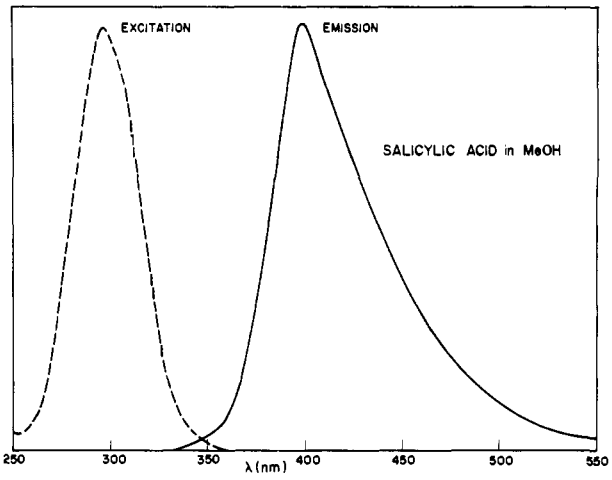


**Figure 9.** Excitation and emission spectra for salicylic acid in methanol. [Sal] = $4 \times 10^{-2}$ mM.

process. However, the *magnitudes* of % $Q$ and $E$ were significantly reduced by the presence of water. Furthermore, at any given value of $\chi$, the magnitude of $E$ in MeOH–$H_2O$ vs. MeOH was decreased by a greater amount than was the magnitude of % $Q$ in MeOH–$H_2O$ vs. MeOH. For example, at $\chi = 2$ the magnitude of $E$ in 10:1 MeOH–$H_2O$ was found to be an order-of-magnitude less than that measured in pure MeOH, whereas the magnitude of % $Q$ was only reduced by about a third in going from 10:1 MeOH–$H_2O$ to pure MeOH. These results may be straightforwardly, but *qualitatively*, accounted for in terms of stronger $Tb^{3+}$–$H_2O$ vs. $Tb^{3+}$–MeOH interactions. The more strongly coordinated water molecules tend to (1) interfere with $Tb^{3+}$–lasalocid interactions and (2) reduce the radiative quantum yields of the excited $Tb^{3+}$ ions. It is also possible that the presence of water causes spectroscopic perturbations by inducing conformational changes in the lasalocid ligand.

**Sal/Tb Excitation and Emission Spectra.** The salicylic acid moiety of the lasalocid molecule is an active (and *direct*) contributor to all of the emission spectra obtained in this study. It is the fluorophore responsible for the intrinsic lasalocid fluorescence, and it is the sensitizer of enhanced terbium luminescence in the NaX/Tb systems. For further characterization of the inherent spectroscopic properties of salicylic acid, by itself and when bound to $Tb^{3+}$, a series of excitation/emission experiments were carried out on free Sal and on Sal/Tb systems in methanol solution. Excitation and emission spectra obtained for salicylic acid in methanol, [Sal] = $4 \times 10^{-2}$ mM, are shown in Figure 9. Data obtained on the quenching of Sal fluorescence (by $Tb^{3+}$) and enhancement of terbium luminescence (by Sal-to-$Tb^{3+}$ energy transfer) are shown in Figures 10 and 11, respectively. Both the quenching and the enhancement experiments were carried out by using near-ultraviolet excitation (into the near-ultraviolet salicylic acid absorption band) on samples of constant absorbance (0.20 optical density units). Equation 1 was used to calculate the percent quenching of Sal fluorescence, and eq 2 was used to calculate the terbium luminescence enhancement factor.

## Discussion

**Lanthanide–Lasalocid Coordination.** The first objective of the present study was to determine if lasalocid A (X537A), when introduced into methanol as a sodium salt, would interact with and possibly coordinate to trivalent lanthanide ions. To probe the existence and nature of lanthanide–lasalocid interactions in methanol, absorption and emission spectra of both the lasalocid and selected lanthanide ions were measured as a function of NaX/Ln concentration ratios. All of the spectroscopic results obtained in this study (and reported under Results) demonstrate strong lanthanide–lasalocid interactions. The absorption spectra of Figure 1 show that $Tb^{3+}$ ions significantly perturb the 308-nm absorption band of lasalocid, and the data plotted in Figure 3 demonstrate that lanthanide ions serve as effective quenchers of

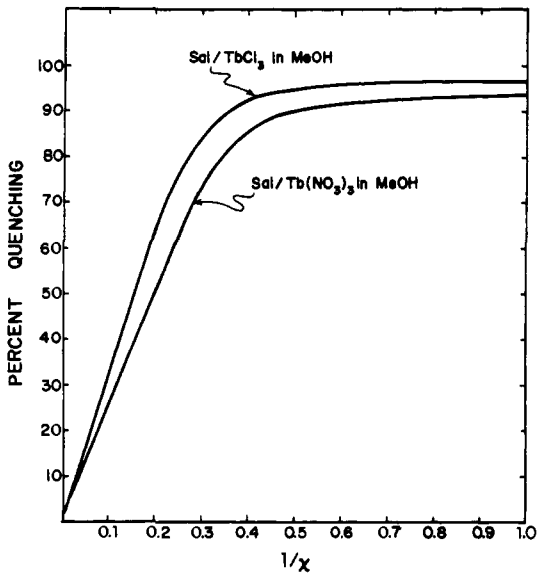


**Figure 10.** Percent quenching (% $Q$) of salicylic acid fluorescence vs. $1/\chi$ = [Tb]/[Sal] for Sal/Tb in methanol. [Sal] was held fixed at $4 \times 10^{-2}$ mM.

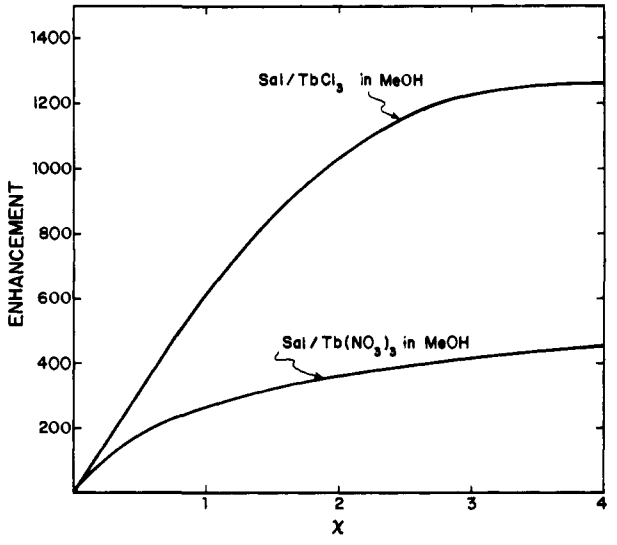


**Figure 11.** Terbium luminescence enhancement ($E$) vs. $\chi$ = [Sal]/[Tb] for $Sal/TbCl_3$ and $Sal/Tb(NO_3)_3$ in methanol solution.

lasalocid fluorescence. The terbium luminescence enhancement data plotted in Figure 4 show that terbium luminescence can be sensitized by remarkably efficient lasalocid-to-$Tb^{3+}$ nonradiative energy-transfer processes, and the neodymium hypersensitive absorption data shown in Figures 7 and 8 provide convincing evidence for strong $Nd^{3+}$–lasalocid interactions. Perhaps the most conclusive evidence for strong and specific lanthanide–lasalocid interactions is provided by the circularly polarized luminescence (CPL) spectra obtained for the NaX/Tb systems (shown in Figure 5). Lanthanide optical activity is generally observable *only* when a chiral ligand is bound *directly* to the $Ln^{3+}$ and is strong *only* when there is some $Ln^{3+}$–ligand multidentate chelation. The additional observation that NaX/Tb CPL persists (albeit, weakly) even in the presence of a strong chelater such as EDTA suggests quite strong $Tb^{3+}$–lasalocid coordination.

The fluorescence quenching data obtained in this study (see Figure 3 and Table I) are not sufficient to prove the formation and long-lived existence of stable and specific lanthanide–lasalocid complexes. Neither are the terbium luminescence enhancement data shown in Figure 4 adequate for this purpose. For a clear differentiation between predominantly "collisional" quenching (involving short-lived $Ln^{3+}$–lasalocid collisional complexes) and quenching due to the existence of long-lived, stable $Ln^{3+}$–lasalocid complexes, fluorescence lifetime data are also required. The shapes of the $E$ (enhancement) vs. $\chi$ curves for NaX/Tb suggest, but do not prove, that $Tb^{3+}$–lasalocid complexation is crucial to the lasalocid sensitization of terbium luminescence process. On the other hand, the absorption spectra of Figures 1 and 7 can *only* be explained on the basis of specific $Ln^{3+}$–lasalocid complexation. Changes in the $Nd^{3+}$ absorption spectrum as a function of [NaX]/[Nd] reflect major alterations within the inner coordination sphere of the $Nd^{3+}$ ion, and changes in the near-ultraviolet absorption band of lasalocid as a function of [NaX]/[Ln] can only be explained in terms of specific $Ln^{3+}$–lasalocid binding. Finally, as was noted above, the most conclusive evidence for specific, coordinative $Ln^{3+}$–lasalocid interactions (i.e., complex formation) is provided by the CPL/emission data on NaX/Tb. Not only are the CPL spectra readily observable in the terbium $^5D_4 \rightarrow {}^7F_5$ emission region, but the luminescence dissymmetry factors $g_{lum}$ observed within this region are moderately large (see Table II). These results suggest that the 4f electrons of the $Tb^{3+}$ in NaX/Tb sense rather strongly the chiral centers of the lasalocid ligands.

Our emission results on the NaX/Ca/Ln systems clearly show that the trivalent lanthanide ions bind to lasalocid rather more strongly than does $Ca^{2+}$. Assuming predominantly noncovalent electrostatic metal ion–lasalocid binding interactions, this observation is most likely accounted for in terms of the greater charge on the $Ln^{3+}$ ions vs. $Ca^{2+}$. Our emission results on the NaX/EDTA/Ln systems show that $Ln^{3+}$–lasalocid coordination persists in the presence of EDTA, although the terbium CPL/emission results on these systems indicate that the coordination is weaker and that the complexes have somewhat different structures. The CPL band shapes change with the addition of EDTA, and the intensities and dissymmetry factors are reduced from the values observed for the corresponding NaX/Tb systems.

The enhancement data shown in Figure 4 and the CPL spectra presented in Figure 5 show that the nature of the anions (other than $X^-$) present in solution has a significant influence on the terbium luminescence from NaX/Tb. Qualitatively, the presence of $Cl^-$ vs. $NO_3^-$ anions appears to have little influence on $Tb^{3+}$–lasalocid coordination. The spectroscopic changes observed in going from chloride to nitrate salts can be attributed primarily to anion-induced perturbations on the *intrinsic* spectroscopic properties of the $Tb^{3+}$ ions rather than to perturbations on the lasalocid ligands or their binding to $Tb^{3+}$. This latter interpretation of anion effects is supported by the additional observation that the quenching of lasalocid fluorescence by $Ln^{3+}$ ions ($Pr^{3+}$, $Nd^{3+}$, $Eu^{3+}$, $Gd^{3+}$, and $Tb^{3+}$) is essentially independent of anion type.

A comparison of our emission results obtained on NaX/Tb in pure MeOH and in MeOH–$H_2O$ mixtures shows that even small amounts of water in solution (as, for example, in a 1000:1 MeOH–$H_2O$ mixture) can reduce $Tb^{3+}$–lasalocid coordination *and* alter the intrinsic spectroscopic properties of the $Tb^{3+}$ ions. This is readily attributable to the somewhat stronger interactions between $H_2O$ and $Tb^{3+}$ vs. MeOH and $Tb^{3+}$.

The results discussed above provide compelling evidence for specific lanthanide–lasalocid coordination (complexation). The next step is to examine these same results for information regarding the nature of this coordination (binding sites and ligand denticity) and the likely stoichiometries of the complexes formed. With regard to binding sites (or ligand donor groups), there can be little question that the carboxylate group of the salicylic acid moiety provides the strongest binding site for the $Ln^{3+}$ ions. This follows from the well-known propensity of $Ln^{3+}$ ions for coordinating to negatively charged oxygen donor groups (and especially to carboxylate groups), and the results obtained in this study support this assertion. Our fluorescence quenching and terbium luminescence enhancement data obtained on the NaX/Ln systems indicate binding at, or near to, the fluorophore and near-ultraviolet chromophore of the lasalocid molecule. This chromophore/fluorophore is the salicylic acid moiety. Furthermore, our fluorescence quenching and terbium luminescence enhancement results on the Sal/Tb systems in methanol (see Figures 10 and 11) show that free salicylic acid does indeed complex to $Tb^{3+}$ in solution.

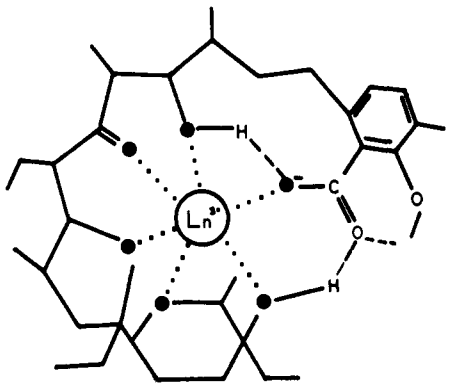


**Figure 12.** Six-coordinate $Ln^{3+}$–lasalocid chelation model with the ligand in a folded conformation. The solid circles denote coordinating oxygen atoms.

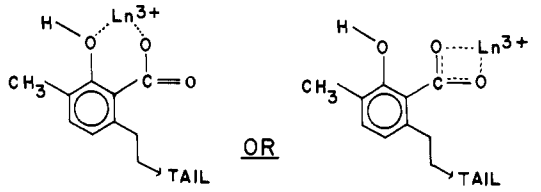


**Figure 13.** Bidentate $Ln^{3+}$–lasalocid chelation structures involving only the salicylic acid head group.

Accepting that the $Ln^{3+}$ ions will bind to lasalocid via $Ln^{3+}$–carboxylate coordination, questions remain regarding other lasalocid donor groups promoting multidentate coordination to a single lanthanide ion or providing multiple binding sites to several lanthanide ions. Excluding the three oxygen atoms in the salicylic acid moiety, the lasalocid molecule contains five other oxygen atoms, each of which is capable of binding to a $Ln^{3+}$. Furthermore, the conformational flexibility of the lasalocid molecule is such that all five of these oxygens can bind to a lanthanide ion already coordinated to the salicylic acid carboxylate group. Folding of the lasalocid molecule into a cyclic conformation such as that shown in Figure 12 can lead to a six-coordinate chelate structure which excludes only two of the eight ligand oxygen atoms from the inner coordination sphere. The structure shown in Figure 12 has, in fact, been found in crystals of the 2:1 lasalocid/$Ba^{2+}$ system.[6] This maximally chelated structure would be ideal for generating lanthanide optical activity (terbium CPL) since it "freezes" the chiral centers of the lasalocid molecule in positions with close proximity to the metal ion. Furthermore, in this structure the $Ln^{3+}$ remains sufficiently close to the salicylic acid chromophore to effect efficient salicylic-acid-to-$Tb^{3+}$ energy transfer and lanthanide ion induced (lasalocid) fluorescence quenching.

Chen and Springer[13] have proposed that the mode of binding for $Pr^{3+}$ to lasalocid ($X537A^-$) in methanol is described by one of the two structures shown in Figure 13. These structures involve bidentate chelation to the metal ion and allow an extended, "open" conformation for the lasalocid molecule. Both of these structures are compatible with efficient salicylic-acid-to-$Tb^{3+}$ energy transfer and lanthanide quenching of lasalocid fluorescence. However, neither of these structures would be expected to generate significant lanthanide optical activity since the chiral centers of the lasalocid ligand are neither "tied down" in a rigid conformational array about the metal ion nor situated "close to" the metal ion. In these structures, the ligand would present a very weak chiral environment ("crystal field") to the lanthanide ion 4f electrons. A distinctive feature of the binding modes represented in Figure 13 is that they are readily compatible with the formation of $Ln^{3+}$–lasalocid bis and tris complexes which dominate at high values of $\chi$ and at the high concentrations used for NMR studies,[13] since only two $Ln^{3+}$ coordination sites are occupied per lasalocid ligand. The chelating mode depicted in Figure 12 can lead to bis complex formation only if the $Ln^{3+}$ is displaced somewhat above the "half-oyster shell" lasalocid conformation, allowing the formation of a 1:2 $Ln^{3+}$–lasalocid sandwich-type complex.

The observation of substantial optical activity (CPL) in the NaX/Tb systems strongly suggests a binding mode involving multidentate chelation in which the chiral centers of the lasalocid ligand are held conformationally rigid. This is satisfied by the chelate structure shown in Figure 12. Comparisons between the CPL data obtained on 1:1 vs. 2:1 NaX/Tb systems (see Figure 5 and Table II) further suggest that the chelate structures, *or* the distribution of chelate types, change with [NaX]/[Tb] concentration ratios. The optical activity observed for the 2:1 system is slightly greater than that observed for the 1:1 system. The terbium luminescence enhancement data plotted in Figure 4 show that the enhancement factor reaches a maximum (and constant) value at $\chi$ = [NaX]/[Tb] = 2, with the values observed at $\chi$ = 1 being about 70% of the maximum value. These terbium CPL and luminescence enhancement results are compatible with a chelate structure model in which chelate structures of the type shown in Figure 12 are the dominant species in 1:1 NaX/Tb solutions and in which bis complexes involving two types of binding modes are formed in 2:1 NaX/Tb solutions. In the proposed 2:1 bis complexes, one lasalocid ligand is bound with the chelate structure of Figure 12, and a second lasalocid ligand binds in a bidentate fashion via its salicylic acid donor groups. In this binding scheme, the six-coordinate ligand is the major contributor to the terbium CPL and luminescence enhancement, while the second ligand makes a lesser contribution to the luminescence enhancement and acts as only a weak perturber on the CPL spectrum. The structural features of the proposed *hetero–bis* complex, and their relationship to the mechanisms assumed to be responsible for the lanthanide optical activity and the lasalocid-to-$Tb^{3+}$ energy transfer processes, are entirely consistent with the observed terbium CPL and luminescence enhancement data on 2:1 NaX/Tb systems. Furthermore, the number of lanthanide coordination sites occupied by lasalocid donor atoms in the proposed hetero–bis complexes is eight—a coordination number quite common in lanthanide coordination chemistry.

The qualitative and small quantitative changes observed in the NaX/Tb CPL spectra in going from the 1:1 to the 1:2 systems suggest that (1) the excess $Tb^{3+}$ is binding at a secondary binding site on the six-coordinate 1:1 Tb(lasalocid) chelate or (2) the six-coordinate 1:1 Tb(lasalocid) chelate is partially unraveled so that the lasalocid ligand (in an "open" conformation) can bind two $Tb^{3+}$ ions. In the former case, a highly likely secondary binding site would be on the salicylic acid head group with the carbonyl oxygen (of the carboxylate group) and the OH group acting as donors.

The dramatic reduction in CPL intensities and luminescence dissymmetry factors observed upon adding EDTA to NaX/Tb solutions suggests complete disruption of the six-coordinate Tb(lasalocid) chelate structures to accomodate the more strongly chelating EDTA ligand in the inner coordination sphere. However, the persistance of weak CPL and the retention of effective (lasalocid) fluorescence quenching indicate that lasalocid remains at least partially bound in the presence of EDTA. Under these conditions, however, the lasalocid is probably bound only via salicylic acid-to-$Tb^{3+}$ coordination.

The fluorescence quenching data plotted in Figure 3 show that maximum quenching (for a given lanthanide ion) does not occur until [Ln]/[NaX] is at least greater than ~0.75. At [Ln]/[NaX] = 0.5 (i.e., a 2:1 NaX/Ln system), the observed quenching values are only about 70% of the maximum values. Assuming bis complexes to exist in the 2:1 NaX/Ln systems, these results can be interpreted in two ways. Microscopically, it is possible that a single $Ln^{3+}$ binding two lasalocid ligands cannot completely quench the fluorescence of both salicylic acid chromophores in its coordination environment. Alternatively, taking complex equilibria into account, only a fraction of the lasalocid molecules are expected to be involved in bis complex formation in 2:1 systems, with the remainder present as free (unbound) species. A combination of these two interpretations most likely provides the best explanation of the quenching results.

The small differences between the quenching results for $Pr^{3+}$, $Nd^{3+}$, $Eu^{3+}$, and $Tb^{3+}$ as well as the larger differences between $Gd^{3+}$ and the other $Ln^{3+}$ ions are most likely due to "electronic" effects rather than to differences in binding constants or chelate structures. By "electronic" effects we refer to the relative 4f-electronic structures of the various $Ln^{3+}$ ions considered here. The 4f-electron states of $Gd^{3+}$ exhibit an energy level structure which is dramatically different from the energy level structures characteristic of $Pr^{3+}$, $Nd^{3+}$, $Eu^{3+}$, and $Tb^{3+}$. If the quenching is dominated by as lasalocid-to-$Ln^{3+}$ energy-transfer mechanism (as it most certainly is in the case of $Tb^{3+}$), then these differences in energy level structures can be expected to show up in the relative quenching efficiencies.

**Lanthanide–Salicylic Acid Coordination.** The data plotted in Figures 10 and 11 demonstrate strong terbium–salicylic acid interactions in methanol solutions of Sal/$TbCl_3$ and Sal/Tb$(NO_3)_3$. In comparing the NaX/$TbCl_3$ quenching data of Figure 3 with the Sal/$TbCl_3$ quenching data of Figure 10, we note the following small differences: (1) at $1/\chi$ values *less* than 0.6, salicylic acid fluorescence is quenched to a significantly greater extent than is lasalocid fluorescence (95% vs. 67% at $1/\chi = 0.5$); (2) maximal quenching in Sal/$TbCl_3$ is ~97% (at $1/\chi = 1$), whereas maximal quenching in NaX/$TbCl_3$ reaches 100% at $1/\chi = 0.85$. The smallness of these differences indicates that the quenching mechanisms operative in the NaX/Tb and Sal/Tb systems are identical or quite similar. The existence of these observed differences can most likely be attributed to structural dissimilarities between the respective complexes which would modulate the quenching processes.

The terbium luminescence enhancement data of Figure 11 demonstrate that the Sal fluorescence quenching mechanism involves, at least in part, Sal-to-$Tb^{3+}$ electronic energy transfer. The differences between these data and the enhancement data presented in Figure 4 for NaX/Tb can most likely be attributed to structural dissimilarities between the terbium–salicylic acid and terbium–lasalocid complexes and differences in the stoichiometries of the dominant complex species present in solution for various $\chi$ values. A significant anion effect ($Cl^-$ vs. $NO_3^-$) appears in the enhancement data for both the NaX/Tb and Sal/Tb systems. The luminescence enhancement for the Sal/Tb systems does not reach a maximum until $\chi \simeq 3$ or 4, suggesting that at least three or possibly four Sal molecules can bind to a single $Tb^{3+}$. Assuming that the $Tb^{3+}$–Sal binding involves bidentate chelation via the Sal carboxylate and hydroxyl groups, the coordination of three or four Sal molecules would lead to total coordination numbers of either six or eight for the $Tb(Sal)_n$ complex at high values of $\chi$. Such coordination numbers are quite common for lanthanide complexes in solution and in the solid state.

**Terbium Luminescence Enhancement.** The sensitization and enhancement of terbium luminescence by irradiation into the near-ultraviolet band of a strongly absorptive ligand chromophore has proved extremely valuable in the use of terbium as a spectroscopic probe of metal binding systems.[24,28] Direct excitation of terbium luminescence can be accomplished with near-ultraviolet or visible radiation, but the luminescence intensities are generally low due to the very low extinction coefficients exhibited by the $Tb^{3+}$ absorptive transitions in these spectral regions. On the other hand, it has been demonstrated that when coordinated to a ligand molecule containing an aromatic near-ultraviolet chromophore, $Tb^{3+}$ acts as a very efficient acceptor in an aromatic chromophore–$Tb^{3+}$ donor–acceptor energy-transfer couple. The absorptive power of the aromatic chromophore combined with the efficiency of this energy-transfer couple leads, in many cases, to significant enhancement of terbium luminescence intensity (over that achieved by direct excitation of the $Tb^{3+}$). The mechanism for the underlying energy-transfer process has not yet been characterized, but empirical observation[21,24,28] suggests that it is relatively short range with critical transfer distances of the order of 8–10 Å.

Assuming a *resonant* energy-transfer mechanism, but making no assumptions regarding the detailed nature of the donor–acceptor interactions (e.g., multipole–multipole vs. exchange), the first major requirement for lasalocid-to-$Tb^{3+}$ energy transfer is significant overlap between the lasalocid fluorescence spectrum and the $Tb^{3+}$ absorption bands. From Figure 2 we see that the lasalocid fluorescence spans the 360–580-nm spectral region with a maximum intensity around 420 nm. On the blue side, this spectrum overlaps the $^7F_6 \rightarrow {}^5D_3$ $Tb^{3+}$ absorption (centered around 380 nm), and on the red side this spectrum overlaps the $^7F_6 \rightarrow {}^5D_4$ $Tb^{3+}$ absorption (centered around 490 nm). The $^7F_6 \rightarrow {}^5D_3$ and $^5D_4$ $Tb^{3+}$ absorption bands are both very narrow, and neither have any significant intensity near the center (and most intense part) of the lasalocid fluorescence spectrum. However, both of these absorption bands are *completely* overlapped by the lasalocid fluorescence band. For efficiency of lasalocid-to-$Tb^{3+}$ energy transfer leading to terbium luminescence, it is especially significant that the terbium $^5D_4$ emitting level can be populated *directly* by a resonant energy-transfer process.

To estimate the efficiency of lasalocid-to-$Tb^{3+}$ energy transfer in the NaX/Tb systems examined in this study, we measured the quantum yield of $Tb^{3+}$ $^5D_4 \rightarrow {}^7F_5$ luminescence under near-ultraviolet irradiation (lasalocid excitation) and the quantum yield of this same luminescence excited at 488 nm (*direct* excitation of the $Tb^{3+}$ $^5D_4$ emitting level). Denoting the former quantum yield by $\Phi_{Tb}(X^-\ \text{exc})$ and the latter quantum yield by $\Phi_{Tb}(Tb^{3+}\ \text{exc})$, the ratio of $\Phi_{Tb}(X^-\ \text{exc})$ to $\Phi_{Tb}(Tb^{3+}\ \text{exc})$ provides an estimate of the lasalocid-to-$Tb^{3+}$ energy-transfer probability. That is,

$$\Phi_{Tb}(X^-\ \text{exc}) = P_{ET}\Phi_{Tb}(Tb^{3+}\ \text{exc}) \qquad (3)$$

where $P_{ET}$ is defined as

$P_{ET}$ = quanta acquired by $Tb^{3+}$ $^5D_4$ emitting level via radiationless energy transfer/quanta absorbed by $X^-$ chromophore

and $\Phi_{Tb}(X^-\ \text{exc})$ is defined as

$\Phi(X^-\ \text{exc})$ = quanta emitted by $^5D_4$ emitting level populated via radiationless energy transfer/quanta absorbed by $X^-$ chromophore

From these definitions, we have

$\Phi_{Tb}(X^-\ \text{exc})/P_{ET}$ = quanta emitted from $^5D_4$ level populated by energy transfer/quanta acquired by $^5D_4$ level by energy transfer

Assuming that the radiative decay of $^5D_4$ is independent of how this level is populated (by either direct radiative excitation or radiationless energy transfer), this latter ratio should be identical with

$\Phi_{Tb}(Tb^{3+}\ \text{exc})$ = quanta emitted from $^5D_4$ level populated by direct radiative excitation/quanta absorbed by $Tb^{3+}$ in direct $^7F_6 \rightarrow {}^5D_4$ excitation

If these relationships hold, then eq 3 is valid and $P_{ET}$ may be considered a *quantum yield of energy transfer.*

Plots of $P_{ET}$ vs. $1/\chi$ for NaX/$TbCl_3$ and NaX/Tb$(NO_3)_3$ very closely resemble the corresponding % $Q$ vs. $1/\chi$ plots. For both NaX/$TbCl_3$ and NaX/Tb$(NO_3)_3$ $P_{ET}$ reaches a maximum value of 0.67 at $1/\chi \simeq 1$. According to the above interpretation of $P_{ET}$, this means that approximately two-third of the near-ultraviolet quanta absorbed by the lasalocid molecule in 1:1 NaX/Tb systems are nonradiatively transferred to the $^5D_4$ emitting level of terbium.

## Conclusions

The results of this study firmly establish that lanthanide ions bind to anionic lasalocid A ($X537A^-$) in methanol and methanol–water solutions. These results also provide clues and qualitative information regarding the structures and stoichiometries of the Ln(lasalocid) complexes formed in methanol. The emission studies on the Tb(lasalocid) systems show that terbium luminescence and lasalocid-to-terbium energy-transfer measurements are especially useful probes for investigating and characterizing

the lanthanide–lasalocid interactions. Although of no *direct* physiological interest, $Tb^{3+}$ should prove to be an excellent spectroscopic replacement probe for the physiologically ubiquitous $Ca^{2+}$ ions in studies devoted to $Ca^{2+}$–lasalocid complexation and transport.

**Acknowledgment.** This work was supported by the National Science Foundation (Grant CHE80-04209) and the Camille and Henry Dreyfus Foundation (through a Teacher–Scholar Award to F.S.R.). The help of Colleen Snavely during the early stages of the work is also gratefully acknowledged.

# The Potential Surface for the Cyclobutadiene Radical Cation

**Weston Thatcher Borden,* Ernest R. Davidson, and David Feller**

*Contribution from the Department of Chemsitry, University of Washington, Seattle, Washington 98195.* *Received March 6, 1981*

**Abstract:** Ab initio calculations on the cyclobutadiene radical cation have been carried out with an STO-3G basis set. At a square geometry the RHF, UHF, and $\pi$ CI energies all depend on whether rectangular or rhomboidal $D_{2h}$ symmetry is imposed on the wave function. The reasons for this undesirable dependency are discussed, and it is shown that inclusion of CI in both the $\sigma$ and the $\pi$ space is necessary to remove it. $\sigma$–$\pi$ CI calculations have been used to determine the optimal rectangular ($b_{1g}$) and rhomboidal ($b_{2g}$) molecular distortions, which are predicted by the Jahn–Teller theorem to result in first-order energy lowering. A rectangular structure is found to correspond to the two minima on the potential surface and a rhomboidal structure to the two transition states, 6.0 kcal/mol higher in energy, that connect the minima. It is shown that, unlike the tetra-*tert*-butyl derivative of cyclobutadiene, the corresponding derivative of the radical cation will not have almost equal bond lengths. Other differences between the neutral molecule and the radical cation are discussed.

Ab initio molecular orbital (MO) theory has proven successful in predicting[1-4] the rectangular equilibrium geometry of cyclobutadiene[5,6] and rationalizing[7] the nearly square geometry of the tetra-*tert*-butyl derivative.[8] In this paper we report the results of calculations on the radical cation of cyclobutadiene.

Two groups have published EPR spectra of tetraalkyl derivatives of the parent radical cation.[9,10] In both cases the hyperfine splitting observed indicated the equivalency on the EPR time scale of all four alkyl groups. This finding is consistent with, but does not demand, an equilibrium geometry in which the four ring carbons are equivalent by symmetry. One of the goals of our theoretical study was to predict the structure of the parent radical cation and, by inference, those of the tetraalkyl derivatives whose EPR spectra have been obtained.

Another objective of this work was to explore the minimal requirements for satisfactory wave functions for the radical cation of cyclobutadiene. Our theoretical studies of diradicals[11] have demonstrated both the importance and the difficulty of obtaining satisfactory wave functions when two electrons must be placed in degenerate or nearly degenerate orbitals. The results of the present study reveal that similar types of problems arise when the degenerate $\pi$ orbitals of square cyclobutadiene are occupied by a single electron.[12]

## Theoretical Considerations

The Jahn-Teller Theorem[13] predicts that the lowest state ($^2E_g$) of the cyclobutadiene radical cation will distort from a square geometry. First-order energy lowering is predicted along $b_{1g}$ and $b_{2g}$ distortion coordinates. The former transforms the square molecule to a rectangle; the latter affords a rhombus.

Since the two distortions are not degenerate, there is no reason to anticipate that they will produce identical energy lowering. In fact, one distortion is expected to lead to two equivalent minima on the potential surface for the lowest state, while the other should lead to two equivalent transition states connecting the minima.[14] The radical cation is therefore expected to pseudorotate about a square geometry, as illustrated in Figure 1. The energy difference between the stationary points along the $b_{1g}$ and $b_{2g}$ coordinates is equal to the energy required for the pseudorotation process.

Optimizing the geometries along the rectangular and rhomboidal distortion coordinates requires calculations in two different $D_{2h}$ subgroups of $D_{4h}$, the point group to which the square molecule belongs. Consequently, two different sets of degenerate ($e_g$) MO's are required for following the $b_{1g}$ and $b_{2g}$ distortions from $D_{4h}$ symmetry. These MO's are shown schematically in Figure 2. At a $D_{4h}$ geometry it should be possible to use either set, since they are related by an orthogonal linear transformation.[15] However, as discussed below, at some levels of calculation the energy will,

(1) Buenker, R. J.; Peyerimhoff, S. D. *J. Chem. Phys.* **1968**, *48*, 354.
(2) Kollmar, H.; Staemmler, V. *J. Am. Chem. Soc.* **1977**, *99*, 3583.
(3) Borden, W. T.; Davidson, E. R.; Hart, P. *J. Am. Chem. Soc.* **1978**, *100*, 388.
(4) Jafri, J. A.; Newton, M. *J. Am. Chem. Soc.* **1978**, *100*, 5012.
(5) Masamune, S.; Souto-Bachiller, F. A.; Machiguchi, T.; Bertie, J. E. *J. Am. Chem. Soc.* **1978**, *100*, 4889.
(6) Whitman, D. W.; Carpenter, B. K. *J. Am. Chem. Soc.* **1980**, *102*, 4272.
(7) Borden, W. T.; Davidson, E. R. *J. Am. Chem. Soc.* **1980**, *102*, 7958.
(8) Irngartinger, H.; Rieglere, N.; Malsch, K. D.; Schneider, K. A.; Maier, G. *Angew. Chem., Int. Ed. Engl.* **1980**, *19*, 211.
(9) Bock, H.; Roth, B.; Maier, G. *Angew. Chem., Int. Ed. Engl.* **1980**, *19*, 209.
(10) Broxterman, Q. B.; Hogeveen, H.; Kok, D. M. *Tetrahedron Lett.* **1981**, *22*, 173.
(11) Review: Borden, W. T.; Davidson, E. R. *Acc. Chem. Res.* **1981**, *14*, 69.
(12) The problems encountered in calculations on the isoelectronic cyclopropenyl radical are related in a general way to those discussed here but differ in detail because of the differences in symmetry and charge between the two systems. The difficulties that arise in the cyclopropenyl radical are discussed in: Davidson, E. R.; Borden, W. T. *J. Chem. Phys.* **1977**, *67*, 2191. See also: Poppinger, D.; Radom, L.; Vincent, M. A. *Chem. Phys.* **1977**, *23*, 437.
(13) Jahn, H. A.; Teller, E. *Proc. R. Soc. London, Ser. A* **1937**, *161*, 220.
(14) See, for instance, the potential surface that appears in: Herzberg, G. "Molecular Spectra and Molecular Structure"; Van Nostrand: New York, 1966; p vol. 3, 44.
(15) Actually, there are infinitely many sets of degenerate MO's that should each give the same energy at a $D_{4h}$ geometry, since each can be expressed as a linear combination of either the rectangular or rhomboidal set. Choice of the appropriate linear combination will result in MO's that are unmixed by a given combination of rectangular and rhomboidal distortions.

0002-7863/81/1503-5725$01.25/0 